




Application of Counter-Wound Multi-Arm Spirals in HTS Resonator Design

Taylor L. Johnston, Arthur S. Edison , Vijaykumar Ramaswamy, Nicolas Freytag, Matthew E. Merritt, Jeremy N. Thomas , Jerris W. Hooker, Ilya M. Litvak, and William W. Brey 

Abstract—Significant sensitivity improvements have been achieved by utilizing high temperature superconducting (HTS) resonators in nuclear magnetic resonance (NMR) probes. Many nuclei such as ^{13}C benefit from strong excitation fields which cannot be produced by traditional HTS resonator designs. We investigate the use of double-sided, counter-wound multi-arm spiral HTS resonators with the aim of increasing the excitation field at the required nuclear Larmor frequency for ^{13}C . When compared to double-sided, counter-wound spiral resonators with similar geometry, simulations indicate that the multi-arm spiral version develops a more uniform current distribution. Preliminary tests of a two-arm resonator indicate that it may produce a stronger excitation field.

Index Terms—Nuclear magnetic resonance, superconducting electronics, superconducting resonators.

I. INTRODUCTION

NUCLEAR magnetic resonance (NMR) is the preeminent technique for determining molecular structures and dynamics in chemistry and biochemistry without sample destruction or extensive sample preparation. However, NMR suffers from intrinsic low sensitivity as a result of the low Boltzmann polarization. Cryogenically cooled NMR probes are commonly used to achieve sensi-

Manuscript received September 28, 2021; revised December 19, 2021 and January 17, 2022; accepted January 18, 2022. Date of publication January 25, 2022; date of current version February 4, 2022. This work was supported in part by NIH/NIGMS under Grants R01GM120151 and P41 GM122698 and in part by the Bruker BioSpin. A portion of the work was done at the National High Magnetic Field Laboratory which is supported in part by the NSF through Cooperative Agreement under Grant DMR-1644779 and in part by the State of Florida. (Corresponding author: William W. Brey.)

Taylor L. Johnston is with the National High Magnetic Laboratory, Tallahassee, FL 32310 USA, and also with the Department of Chemistry and Biochemistry, Florida State University, Tallahassee, FL 32306 USA (e-mail: tjohnston@fsu.edu).

Arthur S. Edison is with the University of Georgia, Athens, GA 30602 USA (e-mail: aedison@uga.edu).

Vijaykumar Ramaswamy and Nicolas Freytag are with the Bruker Switzerland AG, 8117 Fällanden, Switzerland (e-mail: vijaykumar.ramaswamy@bruker.com; nicolas.freytag@bruker.com).

Matthew E. Merritt is with the Department of Biochemistry and Molecular Biology, University of Florida, Gainesville, FL 32601 USA (e-mail: matthewmerritt@ufl.edu).

Jeremy N. Thomas is with the National High Magnetic Field Laboratory, Tallahassee, FL 32310 USA, and also with the Department of Physics, Florida State University, Tallahassee, FL 32306 USA (e-mail: jnt15@my.fsu.edu).

Jerris W. Hooker is with the Department of Electrical and Computer Engineering, FAMU-FSU College of Engineering, Tallahassee, FL 32310 USA (e-mail: hooker@eng.famu.fsu.edu).

Ilya M. Litvak and William W. Brey are with the National High Magnetic Laboratory, Tallahassee, FL 32310 USA, and also with Florida State University, Tallahassee, FL 32306 USA (e-mail: litvak@magnet.fsu.edu; wbrey@magnet.fsu.edu).

Color versions of one or more figures in this article are available at <https://doi.org/10.1109/TASC.2022.3146109>.

Digital Object Identifier 10.1109/TASC.2022.3146109

tivity gains in NMR by reducing the thermal noise from the detection coils and preamplifiers [1]. Further sensitivity improvements have been demonstrated by replacing normal metal resonators in cryogenically cooled NMR probes with high-Q thin-film HTS resonators [2]–[5].

Although ^{13}C NMR detection provides more specific information about molecular structure and identity, biomolecular NMR experiments generally rely on ^1H detection due to the high sensitivity and natural abundance of ^1H . Numerous correlation methods have been developed to use ^1H detection for the study of molecular structures and dynamics, but still there are unsolved challenges resulting from the often significant resonance peak overlap preventing accurate peak identification and quantification. Directly detecting ^{13}C provides significantly improved peak separation but is not widely used due to the relatively low sensitivity and 1.1% natural abundance of ^{13}C . Some biomolecules are primarily comprised of long carbon backbone containing quaternary carbons. Quaternary carbons are challenging to evaluate through indirect ^1H detection experiments due to the absence of attached protons. Direct-detection ^{13}C experiments provide more accurate peak identification and quantification which are especially advantageous in natural products and metabolomics studies [6]–[10].

One challenge with designing ^{13}C HTS resonators is achieving a sufficiently large RF excitation field (B_1) given the limited critical current density in a thin film HTS resonator. Achieving the required transient response in a high-Q HTS resonator has been discussed recently [11]. As the gyromagnetic ratio of ^{13}C is $\frac{1}{4}$ that of ^1H , ^{13}C requires 4x the B_1 field strength to achieve the equivalent nutation angle in the same amount of time. In addition, the increased dispersion that is valuable for peak identification leads to a requirement for even shorter excitation pulses to cover the larger bandwidth. Since the strength of the B_1 field produced is proportional to the total amount of current a resonator can carry, the strength of the B_1 field could be improved by increasing the current capacity of a resonator. We investigate here the use of a counter-wound multi-arm spiral HTS resonator with the aim of achieving an improvement in the B_1 field produced when compared with a traditional single-arm counter-wound spiral resonator.

II. COIL DESIGN

A. HTS Probe Technology

A detailed review of HTS probe construction and technology has been previously published [12]. A key component of HTS probe design is a pair of self-resonant superconductive coils placed on opposite sides of the sample and inductively coupled to both each other and to moveable normal-metal wire loops. Frequency tuning and impedance matching of the resonators are performed by vertical movement of the loops. The coils are oriented parallel to the polarizing (B_0) field to produce a uniform B_1 field and placed as close to the sample as possible. In an all-HTS probe, the pairs of resonators are nested around the sample tube and positioned by priority of detection sensitivity with the outermost coils usually reserved for lock or decoupling channels. Measurements of the

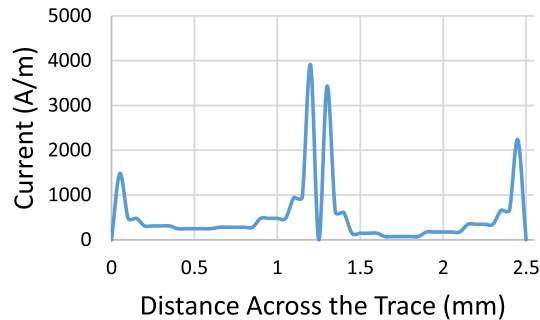


Fig. 1. Current distribution of a 2 turn spiral resonator at sampling location C on the resonator as shown in Fig. 3. The turns are 1.19 mm wide with a 75 μm gap between the turns.

pairwise interactions between resonators can be used to construct a model of the mode structure which facilitates precise tuning of the probe to all required Larmor frequencies [13]. The HTS coils are generally fabricated by photolithographic patterning of thin-film depositions of YBCO on a sapphire planar substrate.

There are several requirements for HTS resonators in NMR probes. The electric field produced by the resonators ideally will not extend into the sample as this will reduce the sensitivity depending on the conductivity of the sample and produce tuning shifts based on the dielectric constant of the sample. The resonators must conform to desired probe specifications including providing a homogeneous B_1 field across the sample, meeting spatial requirements for the probe body, and resonating at the desired frequencies [14]–[15].

A useful class of resonator is a multiturn spiral. At its fundamental resonance frequency, the current along the conductor is a standing wave resulting in nulls at each end [16]. Spirals tend to achieve lower resonance frequencies than single-turn structures and so are most useful when the resonance frequency is relatively low. However, single-sided spiral designs are generally not placed close to the sample due to their large fringing electric field. A second spiral layer added on the other side of the same substrate and wound in an opposite direction creates a structure that traps the fringing electric field within the substrate and produces the desired magnetic field across the NMR sample. This “counterwound spiral” resonator can be placed close to the sample.

When the spiral is used for excitation as well as detection, it is important to maximize the current it carries and the B_1 field it produces. The B_1 field produced by an HTS resonator is limited by its critical current density, J_c . In order to produce the maximum possible B_1 field, the current should be uniformly distributed. A recent study demonstrates that a modified racetrack resonator design provides a more even current distribution by shortening the outer fingers [17]. The current density in a spiral is limited by the standing wave nodes at the ends of the conductor, which we will not address here. However, the current density is also limited by edge effects which cause current to crowd along the inner and outer edges of the resonator [18]. The length and width of the spiral are typically set by the size of the NMR sample, and the trace width is set by the current required for NMR excitation. The number of turns is then determined by what is required to achieve the desired nuclear Larmor frequency. If the number of turns is small, current crowding effects such as shown in Fig. 1 may limit the total current that can be carried by the resonator. We propose to test a resonator design in which number of turns can be adjusted independently of the width of each turn to reduce the current crowding and measure any improvement in its total current capacity.

B. Multi-Arm Spiral Resonator

It has been proposed that multi-arm spiral resonators will have a more uniform current distribution than traditional single-sided spiral resonators [19]. The proposed multi-arm spiral design consists

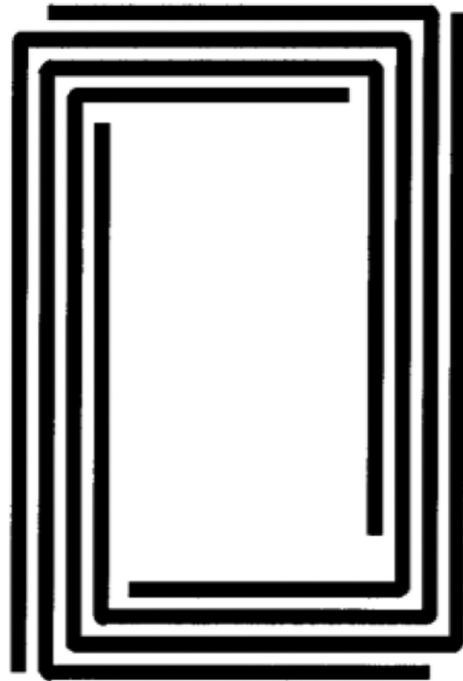


Fig. 2. Schematic drawing demonstrating the coil design of a four-arm spiral.

of nested spiral portions with progressively offset ends as shown in Fig. 2. Increasing the number of arms in the spiral allows the width of the conductors to be adjusted independently of the resonance frequency. By combining the multi-arm design with the concept of counter-wound resonators, the electric field can be trapped within the sapphire substrate which will allow the coil to be placed close to the sample as a detection coil.

III. METHODS

Simple rectangular ^{13}C HTS resonators were designed and simulated to test the effect of the number of turns and number of arms on the current distribution. All resonators had an outer width of 9.45 mm and an inner width of 4.55 mm with a 75 μm gap between the turns within the accuracy of the 50 μm grid in Sonnet. All used a substrate with 0.432 mm thickness and a dielectric constant of 9.9 to approximate sapphire. The coils were designed using the software XIC (Whitely Research Inc.) and exported to the EM simulator, Sonnet (Sonnet Software Inc.). The simulations were performed using a cell size of 0.05 mm. Adjustments were made to the coil design to reach the target resonance frequency of 225 MHz.

A two-arm ^{13}C HTS coil was then designed for experimental comparison with a previously developed ^{13}C resonator [20]. Photolithographic patterning of both coil designs was ordered through Star Cryoelectronics, USA using a YBCO thin-film on sapphire wafer supplied by Ceraco GmbH, Germany.

A. Simulations

The uniformity of the current in the coils was evaluated by using the ratio of the average current to the maximum current. Each coil was sampled from the outer edge of the coil to the inner edge of the coil including the gaps between the conductors. A slice of the data from the simulations was extracted at 4 locations on the coil as shown in Fig. 3. As the coils are double-sided, each side of the coil was sampled individually. The ratios of all 4 locations on both sides was then averaged to produce the ratio of average current to maximum current for each coil under investigation.

B. Experimental Setup

Six resonators each of single-arm and two-arm designs of similar dimensions (a width of 4 mm and height of 19 mm) were fabricated

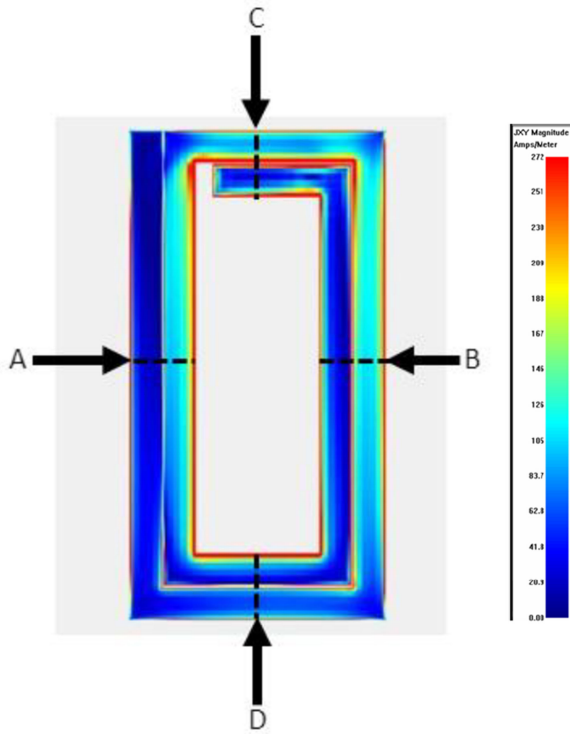


Fig. 3. Single-layer view of simulated current in a coil showing the 4 sampling locations labelled as A, B, C, and D for the current uniformity calculation.

TABLE I
CURRENT UNIFORMITY OF COUNTER-WOUND SPIRAL HTS RESONATORS

Number of Turns	Ratio of Average Current to Maximum Current	Resonance Frequency (MHz)
2	0.13	220
3	0.17	145
4	0.20	100
5	0.20	80

TABLE II
CURRENT UNIFORMITY OF COUNTER-WOUND MULTI-ARM SPIRAL HTS RESONATORS

Number of Arms	Ratio of Average Current to Maximum Current	Resonance Frequency (MHz)
2	0.19	220
4	0.25	220
8	0.26	220

from the same YBCO wafer to obtain the best comparison of these two designs. Due to the cost and difficulty of determining B_1 field strength using NMR, the resonators were tested in a test chamber at 30 K. A low duty cycle ($<10\%$) train of excitation pulses each $40 \mu\text{s}$ in length was used to mimic the requirements of a practical NMR experiment. A first inductive loop was overcoupled to the resonator to reduce the quality factor to 6000 to allow for consistent pulse rise and fall behavior. A second inductive loop was weakly coupled to the resonator to act as a “sniffer” to sample the relative RF magnetic field produced by the resonator. The position of this sniffer loop was kept constant in order to allow for quantitative comparison of the magnetic field by one resonator compared to another. The strength of the RF magnetic field produced by the resonators is considered to

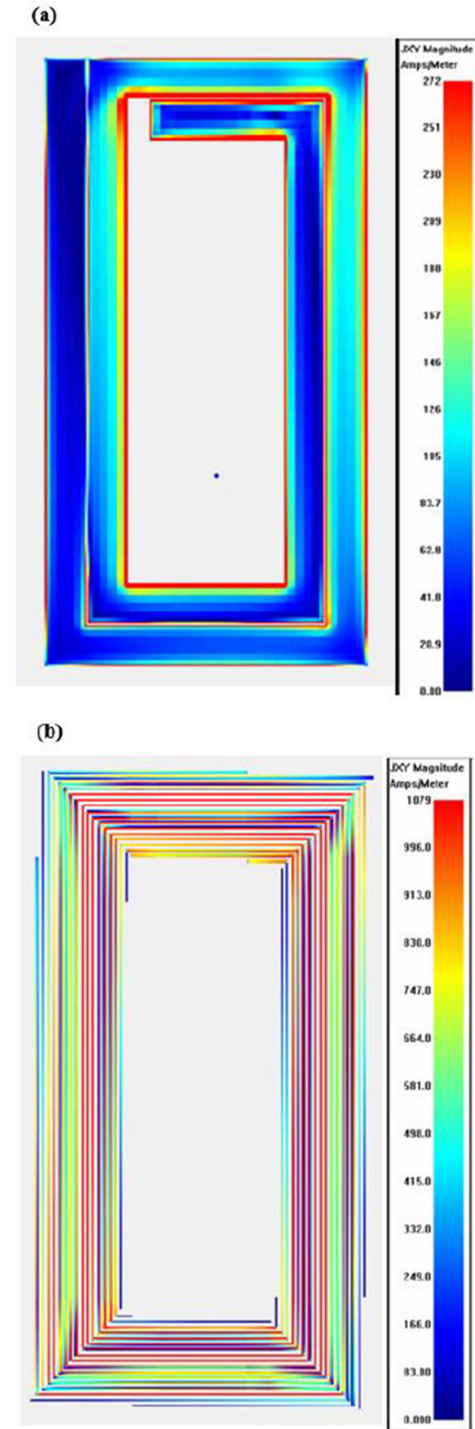


Fig. 4. Simulated current distributions of counter-wound spiral resonators with 9.45 mm width and 18 mm length having the same resonance frequency. One of the two sides is shown (a) Single-arm spiral resonator with 1.19 mm wide turns and $75 \mu\text{m}$ gaps between turns. (b) Eight-arm spiral resonator with $82 \mu\text{m}$ wide turns and $75 \mu\text{m}$ gaps between turns.

be proportional to the strength of the signal from the sniffer loop. To carry out the measurements, we employed a two port vector network analyzer, RF switch and digital pulser in a configuration previously described in [11]. One resonator from the two-arm spiral design and two resonators from the single-arm spiral design were eliminated from the comparison due to poor performance during the RF testing normally associated with defects. The remaining

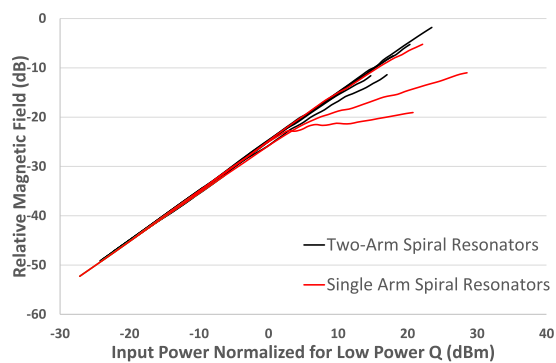


Fig. 5. The saturation behavior of single-arm spiral resonators (red) and two-arm spiral resonators (black).

single-arm spirals had a quality factor range of approximately 10000 to 67000, and the remaining multi-arm spiral resonators had a quality factor range of approximately 20000 to 68000.

IV. RESULTS & DISCUSSION

A series of counter-wound spiral resonators were simulated with varying number of turns. The current uniformity of these coils is summarized in Table I. As the number of turns in the resonator was increased the ratio of average current to maximum current increased indicating decreased current crowding. However, increasing the number of turns in the resonator results in decreased resonance frequency. For higher frequency resonators where a 2-turn spiral is required to meet the target resonance frequency, another method is needed to achieve the B_1 field strength required for ^{13}C experiments.

Several counter-wound multi-arm spiral resonators with varying number of arms were simulated, and the current uniformity of these coils is summarized in Table II. As the number of arms increased, the ratio of average to maximum current increased. As in the case of increasing the number of turns, this reflects a decrease in current crowding. However, as the number of turns for each arm in the multi-arm spiral does not vary with the number of arms, the resonance frequency does not shift.

When comparing simulations of the 2-turn counter-wound spiral resonator to the counter-wound multi-arm spiral resonators, the multi-arm spiral resonators demonstrate an improved current uniformity and are less dominated by edge effects as shown in Fig. 4. The multi-arm spiral resonators demonstrate an improved current uniformity overall with both the 4-arm and 8-arm spirals achieving a 2-fold improvement in the ratio of average current to maximum current compared to the 2-turn counter-wound spiral. This improvement in the ratio of average current to maximum current results in an increased current capacity for the coil. Since the B_1 field strength will be proportional to the current in the coil, the improved current capacity should translate to improved B_1 field strength in the counter-wound multi-arm resonators compared to the 2-turn counter-wound spiral resonator.

We measured the current in single-arm and two-arm counter-wound spiral resonators of similar dimensions. The level of current at which the current density becomes saturated was demonstrated by the saturation behavior of the resonators as a function of current as shown in Fig 5. Although there is considerable scatter in the performance of the resonators arising from typical defects in the HTS films, the multi-arm spiral resonators clearly saturate at a higher magnetic field level than the single-arm spiral resonators. The average 1 dB compression point of the single-arm spiral resonators was approximately $5.1 A_{\text{RMS}}$ compared with greater than $8.2 A_{\text{RMS}}$ for multi-arm spiral resonators.

V. CONCLUSION

A comparative study of the current distribution of counter-wound spiral HTS resonators and multi-arm spiral resonators

demonstrated a more uniform current in the counter-wound multi-arm spiral resonators resulting in the increased B_1 field strength required for ^{13}C NMR experiments. A recently fabricated set of counter-wound spiral HTS resonators and counter-wound multi-arm spiral resonators was compared experimentally to further demonstrate the improved current uniformity and B_1 field strength of counter-wound multi-arm spiral HTS resonators.

REFERENCES

- [1] H. Kovacs, D. Moskau, and M. Spraul, "Cryogenically cooled probes—A leap in NMR technology," *Prog. Nucl. Magn. Reson. Spectrosc.*, vol. 46, no. 2, pp. 131–155, May 2005.
- [2] W. A. Anderson *et al.*, "High-sensitivity NMR spectroscopy probe using superconductive coils," *Bull. Magn. Reson.*, vol. 17, pp. 98–102, 1995.
- [3] H. D. W. Hill, "Improved sensitivity of NMR spectroscopy probes by use of high-temperature superconductive detection coils," *IEEE Trans. Appl. Supercond.*, vol. 7, no. 2, pp. 3750–3755, Jun. 1997.
- [4] W. W. Brey, A. S. Edison, R. E. Nast, J. R. Rocca, S. Saha, and R. S. Withers, "Design, construction, and validation of a 1-mm triple resonance high-temperature-superconducting probe for NMR," *J. Magn. Reson.*, vol. 179, no. 2, pp. 290–293, Apr. 2006.
- [5] V. Ramaswamy, J. W. Hooker, R. S. Withers, R. E. Nast, W. W. Brey, and A. S. Edison, "Development of a ^{13}C -optimized 1.5-mm high temperature superconducting NMR probe," *J. Magn. Reson.*, vol. 235, pp. 58–65, Jul. 2013.
- [6] C. S. Clendinen *et al.*, " ^{13}C NMR metabolomics: Applications at natural abundance," *Anal. Chem.*, vol. 86, no. 18, pp. 9242–9250, Sep. 2014.
- [7] C. S. Clendinen, G. S. Stupp, R. Ajredini, B. Lee-McMullen, C. Beecher, and A. S. Edison, "An overview of methods using ^{13}C for improved compound identification in metabolomics and natural products," *Front. Plant Sci.*, vol. 6, pp. 1–13, Aug. 2015.
- [8] R. E. Patterson *et al.*, "Lipotoxicity in steatohepatitis occurs despite an increase in tricarboxylic acid cycle activity," *Amer. J. Physiol.-Endocrinol. Metab.*, vol. 310, no. 7, pp. E484–E494, Jan. 2016.
- [9] O. Frelin *et al.*, "A directed-overflow and damage-control *N*-glycosidase in riboflavin biosynthesis," *Biochem. J.*, vol. 466, no. 1, pp. 137–145, Jun. 2015.
- [10] M. Ragavan, A. Kirpich, X. Fu, S. C. Burgess, L. M. McIntyre, and M. E. Merritt, "A comprehensive analysis of myocardial substrate preference emphasizes the need for a synchronized fluxomic/metabolomic research design," *Amer. J. Physiol.-Heart Circulatory Physiol.*, vol. 312, no. 6, pp. H1215–H1223, Jan. 2017.
- [11] G. Amouzandeh, V. Ramaswamy, N. Freytag, A. S. Edison, L. A. Hornak, and W. W. Brey, "Time and frequency domain response of HTS resonators for use as NMR transmit coils," *IEEE Trans. Appl. Supercond.*, vol. 29, no. 5, Aug. 2019, Art. no. 1102705.
- [12] V. Ramaswamy *et al.*, "Microsample cryogenic probes: Technology and applications," *eMagRes*, vol. 2, pp. 215–228, Mar. 2013.
- [13] J. N. Thomas *et al.*, "Modeling the resonance shifts due to coupling between HTS coils in NMR probes," in *Proc. J. Phys. Conf. Ser.*, Jun. 2020, vol. 1559, Art. no. 012022.
- [14] N. Sekiya, E. Yoshioka, H. Hoshi, A. Saito, and S. Ohshima, "Design of NMR RF probe constructed with high-temperature superconducting elliptical-coupled resonators," *IEEE Trans. Appl. Supercond.*, vol. 29, no. 5, Mar. 2019, Art. no. 1101504.
- [15] V. Ramaswamy, J. W. Hooker, R. S. Withers, R. E. Nast, A. S. Edison, and W. W. Brey, "Development of a ^1H - ^{13}C dual-optimized NMR probe based on double-tuned high temperature superconducting resonators," *IEEE Trans. Appl. Supercond.*, vol. 26, no. 3, Apr. 2016, Art. no. 1500305.
- [16] N. Maleeva *et al.*, "Electrodynamics of planar archimedean spiral resonator," *J. Appl. Phys.*, vol. 118, 2015, Art. no. 033902.
- [17] O. Sanati *et al.*, " ^{13}C -Optimized HTS NMR RF coil design at 21.1 T," *IEEE Trans. Appl. Supercond.*, vol. 31, no. 5, Aug. 2021, Art. no. 4300305.
- [18] P. Wang, L. Chen, C. Y. Tan, and C. K. Ong, "Analysis of quality factors of spiral resonators," *Microw. Opt. Technol. Lett.*, vol. 48, no. 3, pp. 439–443, Mar. 2006.
- [19] W. H. Wong and I. Feng, "NMR probe with enhanced power handling ability," U.S. Patent 6 590 394 B2, Jul. 8, 2003.
- [20] J. N. Thomas, V. Ramaswamy, I. M. Litvak, T. L. Johnston, A. S. Edison, and W. W. Brey, "Progress towards a higher sensitivity ^{13}C -Optimized 1.5 mm HTS NMR probe," *IEEE Trans. Appl. Supercond.*, vol. 31, no. 5, Aug. 2021, Art. no. 1500504, doi: [10.1109/TASC.2021.3061042](https://doi.org/10.1109/TASC.2021.3061042).